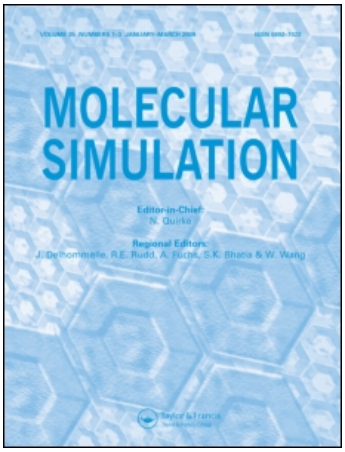

Molecular Simulation
Publication details, including instructions for authors and subscription information:
http://www.informaworld.com/smpp/title~content=t713644482

Molecular modeling of key elastic properties for inhomogeneous lipid bilayers

E. R. May[a]; A. Narang[a]; D. I. Kopelevich[a]
[a] Department of Chemical Engineering, University of Florida, Gainesville, FL, USA

To cite this Article May, E. R. , Narang, A. and Kopelevich, D. I.(2007) 'Molecular modeling of key elastic properties for inhomogeneous lipid bilayers', Molecular Simulation, 33: 9, 787 — 797
To link to this Article: DOI: 10.1080/08927020701308323
URL: http://dx.doi.org/10.1080/08927020701308323

Molecular Simulation, Vol. 33, Nos. 9–10, 15–30 August 2007, 787–797

Taylor & Francis
Taylor & Francis Group

Molecular modeling of key elastic properties for inhomogeneous lipid bilayers

E. R. MAY, A. NARANG and D. I. KOPELEVICH*

Department of Chemical Engineering, University of Florida, Gainesville, FL 32611, USA

(Received January 2007; in final form February 2007)

Fusion and fission of biological membranes play a crucial role in intracellular transport. Until recently, it was believed that membrane shape transformations involved in these processes are driven by proteins. However, recent evidence shows that lipids, by themselves, can drive membrane deformations. It has been hypothesized that the localized formation of certain lipids changes elastic properties of a membrane in such a way that the membrane deforms spontaneously. This study represents a step towards a systematic investigation of the role of various lipids in local changes of membrane elastic properties. We use coarse-grained molecular dynamics (CGMD) simulations to determine possible effects of addition of phosphatidylinositol-4-phosphate (PI4P) lipids on elastic properties of dipalmitoyl phosphatidyl choline (DPPC) lipid bilayers. We investigate the splay (bending) and the molecular tilt moduli of mixed DPPC/PI4P bilayers, as well as the line tension between domains of pure DPPC and mixed DPPC/PI4P bilayers. Although our results indicate negligible effects of PI4P on elastic properties of DPPC bilayers, the developed methodology can be applied to a wide range of lipid systems.

Keywords: Lipid bilayers; Coarse-grained molecular dynamics simulations; Bending modulus; Tilt modulus; Line tension

1. Introduction

Cellular transport processes such as endocytosis, exocytosis and subcellular trafficking involve the budding of vesicles from the donor membrane (fission) and their integration into the membrane of the acceptor compartment (fusion). Both fission and fusion involve pronounced deformation of the membrane and a transient reorganization of its bilayer configuration into highly curved non-bilayer intermediates [1]. Thus, these processes are energetically unfavorable, and do not occur spontaneously—they are under the strict control of specific proteins.

In the classical paradigm, membrane deformation is assumed to be driven entirely by interactions between proteins [2,3]. According to this model, fission is initiated by the recruitment of GTP-binding proteins (ARF and SAR) to the donor membrane. This protein then recruits certain cytosolic proteins called *coat proteins* (COP). The stepwise assembly of COP incrementally deforms the underlying membrane into a spherical shape, ultimately producing a vesicle which is then released along with its encased coat.

Evidence is now accumulating that these proteins do not act alone [4]. They operate in concert with particular membrane lipids, namely, phosphoinositides, diacylglycerol and phosphatidic acid (PA). These key lipids are present in relatively low concentrations within membranes but play a crucial role in the morphological changes. However, the precise role of these lipids is not fully understood. In the literature, there are three models attempting to explain the mechanism by which the lipids participate in membrane deformation.

The first model is the so-called *domain-induced budding model* [5]. There are ample indications for the existence of membrane microdomains *in vivo* that have specific lipid and protein compositions, and model membrane studies have shown that the formation of such membrane microdomains can drive membrane deformation and fission. According to this model, the edge of a membrane domain has an energy proportional to the length of the edge, and membrane bending is a spontaneous process governed by a competition between a decrease in edge energy and an increase in bending energy. Experiments with model membranes have shown

*Corresponding author. Tel.: + 1-352-392-4442. Fax: + 1-352-392-9513. Email: dkopelevich@che.ufl.edu

Molecular Simulation
ISSN 0892-7022 print/ISSN 1029-0435 online © 2007 Taylor & Francis
http://www.tandf.co.uk/journals
DOI: 10.1080/08927020701308323

that formation of microdomains can drive membrane deformation and fission.

The second model, called the *bilayer couple hypothesis*, appeals to the fact that biomembranes are readily bent, but strongly resist area increases [6]. Thus, enzyme-catalyzed changes in the area of one of the leaflets of the membrane can induce dramatic shape changes. The area change can be driven by lipid translocases which move specific lipids from one leaflet to another, thus redistributing the number of lipids in the two leaflets. Experiments show that endocytosis is stimulated by the inward translocation of short chain phosphatidylserine (PS) and phosphatidlyethanolamine (PE) catalyzed by aminophospholipid translocase [7]. Alternatively, it can be mediated by chemical transformation of a specific lipid in one of the leaflets, thus its area. In support of this model, the hydrolysis of phosphatidyl-4,5-bisphophate (PIP_2) in erythrocytes shrinks the inner membrane by $\sim 0.6\%$, and triggers the appearance of "spines" on the surface of the cells [8].

The third model, called the *spontaneous curvature model*, is similar to the bilayer couple hypothesis [4]. This model hypothesizes the existence of an enzyme-catalyzed reaction in which the reactant and product have dramatically different shapes (as opposed to areas in the bilayer couple hypothesis). Cone-shaped lipids ($\bigtriangledown$) cause the membrane to acquire a positive curvature, and inverted-cone-shaped lipids (Δ) cause the membrane to acquire a negative curvature. Thus, the chemical transformation of a molecule from an inverted-cone to a cone will cause the membrane to acquire a positive curvature. Several lines of evidence suggest that the enzyme-catalyzed acylation of lysophosphatidic acid (LPA) to phosphatidic acid (PA) reflects the operation of such a mechanism. For example, it has been found that the activity of brefeldin A ribosylated substrate, an enzyme that catalyzes the conversion of LPA to PA, is essential for fission of tubules in the Golgi body [9]. Moreover, Endophilin I, a protein involved in endocytic membrane fission, has the same enzymatic activity [10]. The validity of this model is also supported by experiments with model membranes involving addition of LPA and PA to bilayers of dioleoyl phosphatidylethanolamine [11].

Although several classes of lipids discussed above have been implicated in membrane deformation, the mechanism by which they induce the shape change is not clear. For instance, it is conceivable that synthesis of PA from LPA changes not only the spontaneous curvature, but also induces line tension at the boundary between domains. Likewise, one can imagine that hydrolysis of PIP_2 to DAG changes not only the area, but also the spontaneous curvature, since diacylglycerol lacks the inositol headgroup of PIP_2. Stated differently, the particular mechanism by which these lipids mediate shape changes cannot be addressed until we know the extent to which the various elastic properties are affected by the lipids. These elastic properties include the spontaneous curvature, the bending modulus, the tilt modulus and the line tension. Although some of the above elastic parameters, such as the bending modulus, have previously been measured both experimentally and from simulations for homogeneous lipid systems [12–14], the information regarding the elastic properties of mixed systems is currently limited.

In the current work, we develop a set of tools that allows one to systematically estimate the elastic properties from molecular dynamics (MD) simulations of inhomogeneous lipid bilayers. These tools are applied to a model system consisting of lipid bilayers containing dipalmitoyl phosphatidyl choline (DPPC) mixed with phosphatidyl-inositol-4-phosphate (PI4P). The choice of the model system is dictated by the fact that phosphatidyl cholines are major components of most biological membranes and that some of the phosphoinositides have been implicated to play an essential role in Golgi membrane functions and related processes of vesicle shape changes [15–18]. Although PI4P has not been directly implicated in these shape change processes, we choose this phosphoinositide in our study due to availability of the experimental data on PI4P headgroup orientation in mixed lipid bilayers [19].

2. Macroscopic model

In this section, we describe the macroscopic theory of membrane deformations with an emphasis on the key parameters of this model which will be obtained from the molecular modeling. The classical model proposed by Helfrich [20] for elastic properties of homogeneous lipid bilayers predicts the following quadratic relationship between the free energy per unit area f and the curvature of the bilayer surface:

$$f = \frac{1}{2}\kappa(C - C_0)^2 + \bar{\kappa}K. \tag{1}$$

Here κ is the bending modulus, C is the mean curvature of a bilayer, C_0 is the spontaneous curvature, $\bar{\kappa}$ is the saddle-splay modulus and K is the Gaussian curvature. Once the model parameters are specified, one can minimize the free energy with respect to the vesicle shapes in order to predict equilibrium vesicle shapes under certain constraints, such as constant volume and surface area [21].

The Helfrich model (1) was further extended by Hamm and Kozlov [22,23] to account for the energy of *tilt* of the lipid molecules. The inclusion of tilt has enabled application of the elastic model to non-bilayer systems such as the hexagonal phase [22] and intermediate stalk of the vesicle fusion [24,25].

The Hamm–Kozlov model assumes that a lipid system can be decomposed into a set of individual lipid monolayers. The tilt of a lipid molecule within a monolayer is directly related to the angle between the normal **N** to the monolayer surface and the director vector **n** of the molecule. The tilt vector **t** is defined as

$$\mathbf{t} = \frac{\mathbf{n}}{\mathbf{n}\cdot\mathbf{N}} - \mathbf{N}, \tag{2}$$

where vectors **N** and **n** are of unit length. The tilt and the bending of a lipid monolayer are captured by the *effective*

total curvature of the chain molecules, defined as the divergence of the director **n** along the monolayer surface,

$$\tilde{J} = \operatorname{div} \mathbf{n}. \tag{3}$$

Note that in the case of the vanishing tilt, the director of the lipids, **n**, coincides with the normal to the surface **N** and the effective total curvature becomes identical to the mean curvature of a monolayer [24],

$$C = \operatorname{div} \mathbf{N}. \tag{4}$$

The explicit inclusion of tilt into the model allows one to account for the changes in the splay energy when the monolayer surface curvature remains constant but the lipids are tilted with respect to the normal to the surface.

Within the framework of the Hamm–Kozlov model, the free energy per unit area of a lipid monolayer is given by

$$f = \frac{1}{2}\kappa(\tilde{J} - \tilde{J}_s)^2 + \bar{\kappa}\tilde{K} + \frac{1}{2}\kappa_\theta t^2, \tag{5}$$

where κ is the splay modulus of the monolayer, $\tilde{J}_s$ is the spontaneous total curvature, $\bar{\kappa}$ is the Gaussian modulus, $\tilde{K}$ is the Gaussian curvature (modified to account for tilt contributions), and κ_θ is the tilt modulus. The total energy of a microstructure is a sum of energies of all monolayers comprising it.

As discussed in the Introduction, it is believed that certain lipids are localized within rafts (domains). The existence of domains of different lipid composition within a membrane is expected to cause interfacial (line) tension between these domains [26], which needs to be accounted for in the energetic model. Therefore, the total energy of a bilayer is assumed to be

$$F = \sum_k \int_{A_k} f \mathrm{d}A + \sum \sigma \int_{\partial A_k} \mathrm{d}l. \tag{6}$$

Here, the first term corresponds to the free energy of the k-th domain A_k of uniform composition within the lipid bilayer and the second term corresponds to the energy of the line tension between these domains.

It should be noted that the three theories described in the Introduction are subsumed by the model equations (5) and (6). For example, the *domain-induced budding* model will be exhibited by the line tension at the domain boundaries and differences in the splay modulus within different domains. The *bilayer couple hypothesis* will be exhibited by the difference in the spontaneous total curvature and splay moduli of the two leaflets of the bilayer. The notion of the spontaneous total curvature also allows one to describe the *spontaneous curvature model*.

In what follows we consider bilayers with equal concentrations of different lipids in the different leaflets. Therefore, the bilayer spontaneous total curvature is $\tilde{J}_s = 0$. Moreover, the contributions of the Gaussian curvature term to the bilayer free energy can be neglected. Therefore, to completely describe the membrane, it suffices to obtain the bending modulus κ, the tilt modulus κ_θ, and the line tension coefficient σ.

3. Simulation details

In order to accurately evaluate the elastic (i.e. macroscopic) properties using microscopic simulations, it is necessary to perform simulations of systems containing thousands of lipids for hundreds or thousands of nanoseconds. The application of a detailed atomistic model to such length- and time-scales is extremely time-consuming even with modern computing systems and therefore limits the scope of the systems that can be investigated within a reasonable time frame. Therefore, simulations of lipid systems often employ less detailed models, such as the Brownian dynamics simulations [27], dissipative particle dynamics [28], and coarse-grained molecular dynamics (CGMD) models [29–33]. In the current work, we use a CGMD model, which allows one to perform simulations on nearly atomic length scales, while reducing the computational time by orders of magnitude and therefore allowing exploration of the systems on sufficiently large time- and length-scales. The CGMD models approximate small groups of atoms by a single united atom (bead). Several such models have been introduced and applied to simulations of various complex molecular systems [29–32,34,35,].

In this work, we use the coarse-grained model proposed by Marrink *et al.* [32]. This model has been shown to yield good agreement with experiments and atomistically-detailed simulations for such quantities as density and elasticity of pure lipid bilayers. Within this model, for example, four methylene groups of lipid tails are represented by a single hydrophobic coarse-grained bead (denoted as C) and four water molecules are represented by a single spherical polar bead (denoted as P). This model also provides several types of beads that can be used to model various groups of atoms (such as glycerol and phosphate) within lipid headgroups. The interactions between non-bonded beads are modeled by the Lennard–Jones (LJ) potential. The LJ radius $r_0 = 0.47\,\mathrm{nm}$ is assumed to be the same for all beads, whereas the energy parameter ε of the LJ potential is chosen depending on the nature of the interacting beads. For example, $\varepsilon = 5\,\mathrm{kJ/mol}$ for hydrophilic attraction between polar P beads, and $\varepsilon = 1.8\,\mathrm{kJ/mol}$ for a repulsive interaction between hydrophobic apolar (C) and hydrophilic polar (P) beads. Electrostatic interactions between the charged beads are modeled by a shifted coulombic potential. The shift mimics distance-dependent screening effects and is performed smoothly from 0 kJ/mol to 0 at the cut-off radius of 1.2 nm. For chemically-bonded beads, the bond length vibration is modeled by a harmonic potential with an equilibrium bond length of 0.47 nm and a force constant of $1250\,\mathrm{kJ\,mol^{-1}\,nm^{-2}}$. The bond angle vibrations are modeled by the harmonic potential of cosine type. The equilibrium force constant is $25\,\mathrm{kJ\,mol^{-1}}$ for bond angles of the molecules considered in the current work. The equilibrium bond angles depend on the geometry of the molecule. For example, the equilibrium value of all bond angles in the DPPC and PI4P lipid tails is 180°.

All MD simulations reported in this paper are performed using the GROMACS simulations package [36]. In this work, we investigate the elastic properties of lipid bilayers consisting of DPPC and phosphatidylinositol-4-phosphate (PI4P) lipids. The detailed atomistic structures and the corresponding coarse-grained representations of some of these lipid molecules are shown in figure 1. The coarse-grained models for DPPC lipids and water molecules are taken directly from Ref. [32]. A coarse-grained model for the PI4P lipid is developed using the methodology proposed in Ref. [32] for mapping different functional groups within a molecule to coarse-grained beads with specific properties. The phosphate groups of PI4P are modeled as charged beads acting as hydrogen bond acceptors (denoted as Qa) and the inositol ring is modeled as a single polar bead P due to its ability to form hydrogen bonds and its high solubility in water. The charges of the upper and lower phosphate groups are $-2e$ and $-e$, respectively. The model for tail chains is identical to that of DPPC.

The equilibrium bond angles for PI4P headgroup are chosen as follows: Angle P—Qa—Na = 180°, angle Qa—Na—Na = 120° and angle Qa—Na—C = 180°. There is no angle-dependent potential imposed on the vibrations of the angle Qa—P—Qa, similarly to the absent angle-dependent potential for the Q_0—Qa—Na angle in the DPPC model [32].

This choice for the Qa—P—Qa angle is motivated by the experimental observation that for PI4P molecules contained in a lipid bilayer the inositol ring of PI4P is not normal to the bilayer, but becomes tilted towards the bilayer [19]. It has been speculated that this structural feature of PI4P is caused by the electrostatic interaction between the negatively-charged phosphate group of PI4P and the positively-charged choline group of a major component of the bilayer. In order for this attraction to manifest itself in the tilting of the PI4P headgroup, the angle Qa—P—Qa has to be sufficiently flexible and therefore we do not impose any potential on this angle. Our simulations confirm that this choice for the Qa—P—Qa angle provides the necessary flexibility of the PI4P headgroup. The probability distributions of the values of the Qa—P—Qa angle for PI4P contained in a DPPC bilayer at several different concentrations are shown in figure 2. All of the systems display the same trend with a peak in probability at ≈ 2.1 radians. Therefore, the upper phosphate group is being pulled down towards the bilayer–water interface in a qualitative agreement with the experiments.

We note that the model for PI4P can be further improved. In particular, currently we use a single coarse-grained bead to model a rather bulky inositol ring and perhaps it would be more realistic to model this ring by a larger bead. However, in the current work we try to introduce as little of new features to the coarse-grained model of Ref. [32] as possible.

The simulation time of the coarse-grained model is on average four times faster than the real time [32]. Therefore, the length of simulations is reported below in terms of the real time (equal to the simulation time multiplied by four). The bilayer systems were prepared by self-assembly. Self-assembly simulations of DPPC and PI4P were conducted at relative PI4P concentrations of 0, 5, 10 and 20%. Initially, the self-assembly was performed for 200 lipid molecules at the proper relative concentrations and 28 water molecules (seven coarse-grained water beads) per lipid. The systems were then simulated at a temperature of 298 K for a time of 800 ns, during which a bilayer formed and equilibrated. The bilayer system was then copied laterally four times to create a new bilayer system consisting of 800 lipid molecules. The 800 lipid bilayer was then simulated for 1.6 μs at 298 K. The final configuration of the 800 lipid system was then copied laterally four times to create a 3200 lipid system.

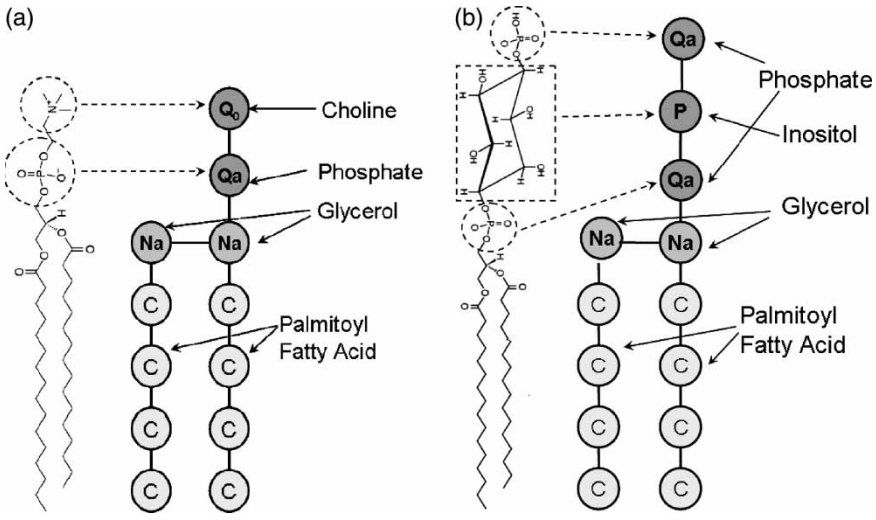

Figure 1. Detailed atomistic structures and the corresponding coarse-grained models of: (a) DPPC, and (b) PI4P lipids. Mapping between different groups of atoms and the coarse-grained beads is shown for some groups. The bead types are denoted as follows: C, apolar, P, polar, Qa (Na), charged (non-polar) groups acting as a hydrogen bond acceptor, Q_0, charged groups with no hydrogen bonding capabilities (see Ref. [32]).

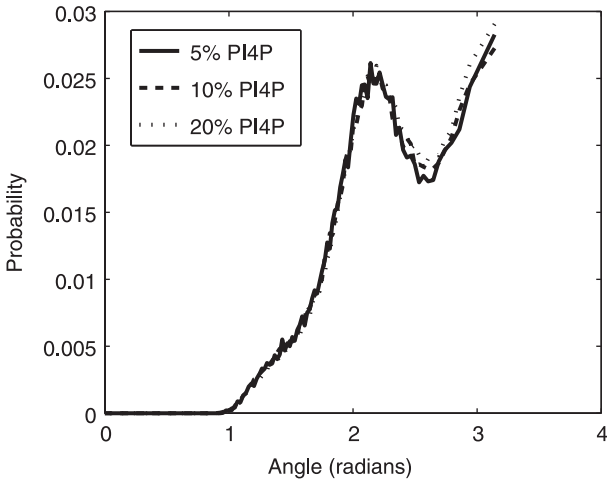

Figure 2. Probability distribution of the angle Qa—P—Qa of the PI4P molecules contained in DPPC bilayers at concentrations of 5, 10 and 20%.

Additional water was placed in the simulation box to bring the relative hydration level up to 78 water molecules (19.5 coarse-grained water beads) per lipid. These 3200 lipid systems were simulated at 298 K for 1.2 μs. The temperature was then raised to 323 K and the system was equilibrated for an additional 800 ns. The equilibration was followed by a production run for 1.2 μs whose results were used in the analysis of the system. In all the simulations reported here, we used the Berendsen temperature and anisotropic pressure coupling schemes [37]. The pressure in the system was maintained at one bar.

4. Calculations of macroscopic elastic properties from molecular dynamics simulations

As discussed in Section 2, in order to describe the elastic properties of a lipid bilayer composed of symmetric monolayers it is necessary to obtain the following parameters: the splay modulus κ, the tilt modulus κ_θ, and the coefficient σ of line tension between domains of different lipid composition. Below we discuss calculation of these parameters from MD simulations.

4.1. Splay and tilt moduli of a monolayer

4.1.1. Method of calculation. The splay and tilt moduli are obtained from a statistical analysis of equilibrium MD simulations. The method is a generalization of a well established procedure for calculation of a bending modulus of a flat bilayer [13,38] based on measuring the fluctuations of a membrane and fitting the amplitude of these fluctuations to the predictions of the Helfrich elastic model equation (1).

In this section, we will consider a homogeneous monolayer, i.e. a monolayer with no rafts and therefore no line tension between the rafts. Moreover, the bilayer is assumed to be composed of two identical monolayers. Within the framework of the Hamm–Kozlov model equation (5), the energy of this bilayer is equal to twice the energy of an individual monolayer, which in turn is given by

$$F = \frac{1}{2}\int [\kappa \tilde{J}(x,y) + \kappa_\theta t^2(x,y)]\mathrm{d}x\mathrm{d}y. \tag{7}$$

Here, the bilayer is assumed to be parallel to the $x-y$ plane, and we took into account the facts that the spontaneous total curvature of a homogeneous bilayer vanishes and the contribution of the Gaussian curvature term to the bilayer energy is negligible. When the fluctuations of the bilayer are sufficiently small, the effective total curvature is approximated to the leading order by

$$\tilde{J}(x,y) = \frac{\partial^2 h}{\partial x^2} + \frac{\partial^2 h}{\partial y^2} + \frac{\partial t_x}{\partial x} + \frac{\partial t_y}{\partial y}, \tag{8}$$

where $h(x,y)$ is the function defining the bilayer surface, and t_x, t_y are the x- and y-components of the tilt vector.

Further analysis of the membrane fluctuation magnitude is performed in the Fourier space. Let us define vector

$$\mathbf{f}(\mathbf{q}) \equiv (\hat{h}(\mathbf{q}), \hat{t}_x(\mathbf{q}), \hat{t}_y(\mathbf{q})),$$

where $\mathbf{q}$ is the wavevector,

$$\hat{h}(\mathbf{q}) = \frac{1}{\sqrt{S}}\int h(x,y)\mathrm{e}^{-i(q_x x + q_y y)}\mathrm{d}x\mathrm{d}y \tag{9}$$

is the Fourier transform of the function $h(x, y)$ specifying the bilayer surface, and similarly $\hat{t}_x(\mathbf{q})$, $\hat{t}_y(\mathbf{q})$ are the Fourier transforms of the x- and y-components of the tilt vector $\mathbf{t}(x, y)$. S in equation (9) denotes the monolayer area. Then the monolayer energy equation (7) can be rewritten as:

$$F(\mathbf{f}) = \frac{1}{2}\sum_{\mathbf{q}} \mathbf{f}(\mathbf{q})\cdot\mathbf{A}(\mathbf{q})\mathbf{f}(\mathbf{q}), \tag{10}$$

with matrix $\mathbf{A}(\mathbf{q})$ given by

$$\mathbf{A}(\mathbf{q}) = \begin{pmatrix} \kappa q^4 & -i\kappa q^3\cos\phi & -i\kappa q^3\sin\phi \\ i\kappa q^3\cos\phi & (\kappa q^2\cos^2\phi + \kappa_\theta) & \kappa q^2\cos\phi\sin\phi \\ i\kappa q^3\sin\phi & \kappa q^2\cos\phi\sin\phi & (\kappa q^2\sin^2\phi + \kappa_\theta) \end{pmatrix}. \tag{11}$$

Here and below it will be convenient to use polar coordinates for the wavevector $\mathbf{q} = (q_x, q_y) = (q\cos\phi, q\sin\phi)$. Since the matrix $\mathbf{A}(\mathbf{q})$ is self-adjoint for each value of the wavevector $\mathbf{q}$, we can rewrite the inner products in equation (10) using the normal coordinates,

$$F(\mathbf{g}) = \frac{1}{2}\sum_{\mathbf{q}}\sum_{j=1}^{3} \lambda_{\mathbf{q},j}|\mathrm{g}_j(\mathbf{q})|^2. \tag{12}$$

Here $\lambda_{\mathbf{q},j}$ are the eigenvalues of the matrix $\mathbf{A}(\mathbf{q})$ and the normal coordinates $\mathbf{g}(\mathbf{q})$ are defined by the equation

$$\mathbf{g}(\mathbf{q}) = \mathbf{U}^{-1}(\mathbf{q})\mathbf{f}(\mathbf{q}), \tag{13}$$

where $\mathbf{U}(\mathbf{q})$ is an orthogonal matrix whose columns are eigenvectors of matrix $\mathbf{A}(\mathbf{q})$. Since the probability $P(\mathbf{g})$ of observing a monolayer in a configuration $\mathbf{g}$ is given by the Boltzmann distribution, $P(\mathbf{g}) \propto \exp(-F(\mathbf{g})/k_BT)$, we obtain using equation (12)

$$\langle g_j(\mathbf{q})\rangle = 0, \quad \langle g_j(\mathbf{q})g_{j'}(\mathbf{q}')\rangle = \delta_{j,j'}\delta_{\mathbf{q},-\mathbf{q}'}\frac{k_BT}{\lambda_j(\mathbf{q})}. \tag{14}$$

Substituting equation (14) into equation (13), we obtain

$$\langle \mathbf{f}(\mathbf{q})\rangle = 0, \quad \langle \mathbf{f}(\mathbf{q})\mathbf{f}(\mathbf{q}')\rangle = \delta_{\mathbf{q},-\mathbf{q}'}k_BT\mathbf{A}^{-1}(\mathbf{q}). \tag{15}$$

In particular, since

$$\mathbf{A}^{-1}(\mathbf{q}) = \begin{pmatrix} \left(\frac{1}{\kappa q^4} + \frac{1}{\kappa_\theta q^2}\right) & \frac{i\cos\phi}{\kappa_\theta q} & \frac{i\sin\phi}{\kappa_\theta q} \\ -\frac{i\cos\phi}{\kappa_\theta q} & \frac{1}{\kappa_\theta} & 0 \\ -\frac{i\sin\phi}{\kappa_\theta q} & 0 & \frac{1}{\kappa_\theta} \end{pmatrix} \tag{16}$$

we obtain

$$\langle|\hat{t}_x(\mathbf{q})|^2\rangle = \langle|\hat{t}_y(\mathbf{q})|^2\rangle = \frac{k_BT}{\kappa_\theta} \tag{17}$$

and

$$\langle|\hat{h}(\mathbf{q})|^2\rangle = k_BT\left(\frac{1}{\kappa|\mathbf{q}|^4} + \frac{1}{\kappa_\theta|\mathbf{q}|^2}\right). \tag{18}$$

Therefore, in order to obtain the splay and tilt moduli, κ and κ_θ, it is necessary to measure the spectral intensities $|\hat{h}(\mathbf{q})|^2$ and $|\hat{\mathbf{t}}(\mathbf{q})|^2$ of the fluctuations of the monolayer surface $h(x,y)$ and the molecular tilt $\mathbf{t}(x, y)$. We define the monolayer surface $h(x, y)$ as a surface passing through the bonds connecting the glycerol and the phosphate groups of each of the lipid molecules. Recall that in order to obtain the tilt vector of the lipids, it is necessary to obtain the normal $\mathbf{N}(x, y)$ to the monolayer surface and the lipid director vector $\mathbf{n}$. In order to compute the derivatives of the monolayer surface that are required to obtain the normal vector $\mathbf{N}$, we perform differentiation of the Fourier series for the monolayer surface $h(x, y)$.

Since a lipid molecule has a large number of degrees of freedom, there is no unique definition for its director $\mathbf{n}$. In the current work, we have investigated four possible definitions of the director vectors. In all cases, the director is defined as a vector connecting two points representing locations of the lipid tail and the headgroup. The tail location is defined to be either (1) the center of mass of all the tail beads; or (2) the average between the locations of the last beads of the two tails of a lipid molecule. The headgroup location is defined as either (1) the center of mass of all headgroup beads; or (2) as a mid-point of a bond connecting the phosphate and the glycerol beads of a lipid.

4.1.2. Results. The spectral intensities of the tilt fluctuations are shown in figure 3 for the four different definitions of the director vector $\mathbf{n}$ discussed above. The fluctuations are shown for a range of PI4P concentrations in the DPPC bilayer. As it can be seen, the spectral intensity of the tilt fluctuations is virtually independent of the PI4P concentration and is somewhat more dependent on the precise definition of the tilt vector. A systematic deviation of the tilt magnitude fluctuations

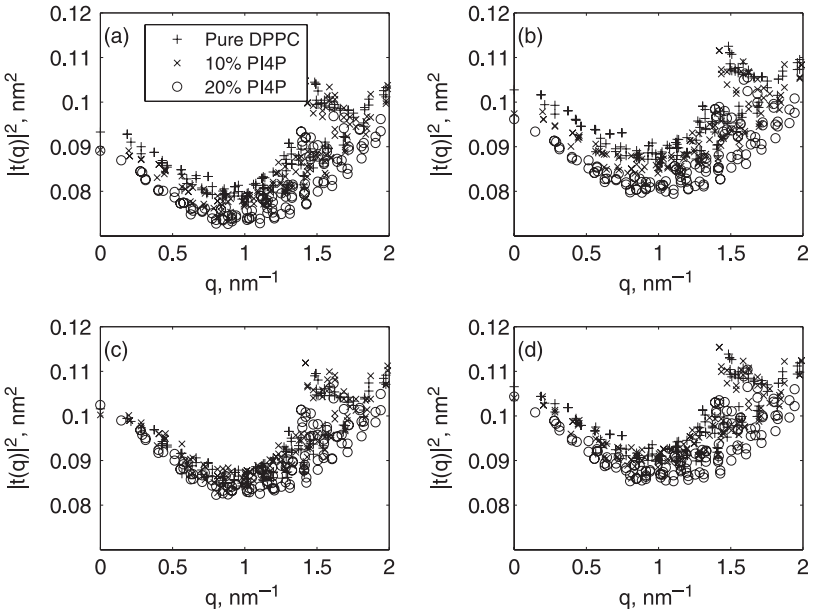

Figure 3. Spectral intensity of tilt fluctuations for pure DPPC bilayers and for DPPC bilayers containing 10 and 20% of PI4P. Subplots (a)–(d) show the tilt fluctuations obtained with the four different definitions of the molecular director vector $\mathbf{n}$ discussed in text: (a) 1–1, (b) 1–2, (c) 2–1, and (d) 2–2, where $i - j$ denotes the director definition corresponding to the i-th definition of the headgroup location and the j-th definition of the tail location.

from a constant predicted by equation (17) is also observed. However, to a good degree of approximation, the tilt fluctuations are independent of the wavevector and from equation (17) we obtain the tilt modulus $\kappa_\theta \approx 48.5\,\mathrm{mN/m}$ for all considered PI4P concentrations. We note that this value is in good agreement with the theoretical estimate, $\kappa_\theta \approx 50\,\mathrm{mN/m}$, of Hamm and Kozlov [23] based on a crude molecular model and with their estimate $\kappa_\theta \approx 40\,\mathrm{mN/m}$ based on an analysis of experimental data for DOPE phospholipid phases.

The spectral intensity of the surface fluctuations is shown in figure 4. It is clear that for all considered PI4P concentrations the surface fluctuations are the same. Therefore, it follows from equation (18) that the splay modulus is also independent of the PI4P concentration.

A least squares fit of the measured spectral intensity to equation (18) is shown by the solid line in figure 4. Good agreement between the model prediction and the bending fluctuations measured from the experiments indicates that the Hamm–Kozlov model (5) adequately describes the membrane fluctuations for the entire range of the considered wavevectors q. The least squares fit yields the value $\kappa \approx 1.9 \times 10^{-19}\,\mathrm{J}$ of the bending modulus. This value is somewhat larger than the values $\kappa \approx 4 \times 10^{-20}\,\mathrm{J}$ obtained in the earlier atomistic [13] and coarse-grained simulations [32] of DPPC membranes. This discrepancy can be explained by the fact that these earlier results were obtained by fitting the bilayer fluctuation intensity to a model that neglects the contributions of the tilt fluctuations. In fact, when we neglect the tilt modulus in equation (18) and perform the least-squares fit of the spectral intensities corresponding to the long wavelength fluctuations with $q \leq 1\,\mathrm{nm}^{-1}$, we obtain $\kappa = 5.8 \times 10^{-20}\,\mathrm{J}$, which is in a closer agreement with the value obtained in Refs. [13,32].

Moreover, the value $\kappa = 1.9 \times 10^{-19}\,\mathrm{J}$ obtained from our fit to the equation (18) is rather close to the upper experimental estimate $\kappa \approx 1.2 \times 10^{-19}\,\mathrm{J}$ for unsaturated phosphatidyl choline membranes [39]. Since in the current work we considered a saturated DPPC molecule and the results of [39] indicate that the bending modulus increases with the degree of saturation, it is expected that the value of the bending modulus obtained from our simulations is even closer to the experimental values. This interplay of the membrane bending and the lipid tilt fluctuations and the corrections to the bending modulus arising from the molecular tilt will be explored in further details in a separate publication [40].

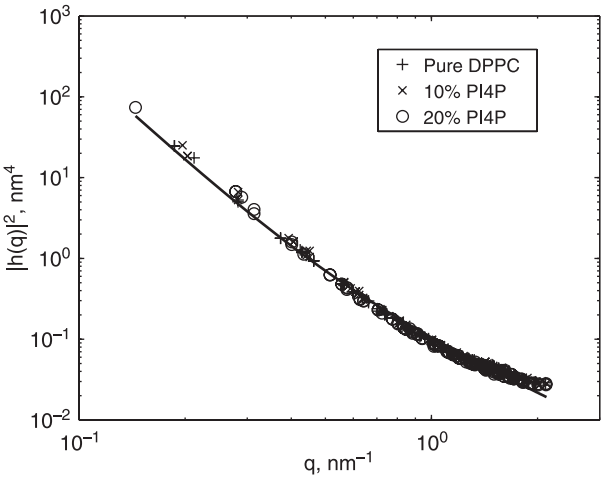

Figure 4. Spectral intensity of bilayer surface fluctuations for pure DPPC bilayers and for DPPC bilayers containing 10 and 20% of PI4P. Results of the least-squares fit to equation (18) are shown by the solid line.

4.2. Line tension

Another important factor in the elastic properties of the biomembranes is the line tension between the domains (rafts) of different lipid concentration. Recall that the line tension is defined as the free energy per unit length of the area dividing two domains [26], see also equation (6). Line tension between two domains of lipids with different tail lengths has been recently estimated analytically [41] using the Hamm–Kozlov functional (5) and taking into account the change in the lipid tilt in the neighborhood of the domain boundary in order to accommodate the change in the bilayer thickness due to the change in the length of the incompressible lipid tails. However, the effect of varying lipid *headgroup* properties on the line tension has not been fully investigated. In addition, it is of interest to investigate the line tension between domains containing different mixtures of lipids. In what follows, we compute the line tension between domains containing only DPPC and a DPPC/PI4P mixture.

4.2.1. Method of calculation. The line tension can be thought of as a two-dimensional (2d) analogue of the surface tension between two liquids. This similarity allows us to modify the methods developed for estimation of the surface tension from MD simulations [42] and apply them to the calculation of the line tension.

Consider a flat membrane. Assume that this membrane lies in the $x - y$ plane and that the thickness of the membrane is $2h$, i.e. in the z-direction the membrane is bounded between $z = -h$ and $z = h$. Let us now define a 2d analogue of the pressure tensor. For this, let us consider the three-dimensional (3d) pressure tensor P. A component $P_{\alpha\beta}$ of this tensor corresponds to the force per unit area in the direction β exerted on a plane with the normal pointing in the direction α (α, $\beta = x$, y or z). Integrating $P_{\alpha\beta}$ in the direction z normal to the bilayer surface, we obtain

$$P^{2\mathrm{d}}_{\alpha\beta}(x,y) = \int_{-h}^{h} P_{\alpha\beta}(x,y,z)\mathrm{d}z, \quad \alpha,\beta = x,y. \tag{19}$$

Here, $P^{2\mathrm{d}}_{\alpha\beta}(x,y)$ is the 2d pressure tensor whose components are the averaged forces per unit length in the direction β exerted on a *line* on the bilayer surface with the normal pointing in the direction α. In what follows we assume that the shear forces are negligible, i.e. that the off-diagonal

terms of the pressure tensor are zero, $P^{2d}_{\alpha\beta} = 0$ for $\alpha \neq \beta$, and focus on calculations of the diagonal elements of the 2d pressure tensor.

The bilayer is isotropic away from the boundary between the domains. Hence, the 2d pressure tensor is isotropic away from the boundaries and $P^{2d}_{xx} = P^{2d}_{yy}$ as illustrated in insets (a) and (b) of figure 5. However, near the domain boundaries, the 2d pressure tensor becomes anisotropic, see inset (c) of figure 5. Assume for definiteness that the domain boundary is parallel to the y-axis. Then the x-component of the 2d pressure tensor remains constant (in order to maintain the balance of forces in the normal direction) whereas the y-component changes and this change accounts for the line tension,

$$\sigma = \int_{x_1}^{x_2} \left(P^{2d}_{xx} - P^{2d}_{yy} \right) \mathrm{d}x. \tag{20}$$

Here, the integration is performed over a sufficiently large interval in x such that the 2d pressure tensor becomes isotropic when x is outside the interval $[x_1, x_2]$.

The pressure tensor is obtained from the MD simulations using the virial theorem [42]. It is well known that there are two contributions to the pressure tensor P: the kinetic pressure tensor P^K which accounts for effects of molecular kinetic energy and the configurational pressure tensor P^C which accounts for contributions of potential interactions [43],

$$P_{\alpha\beta} = P^K_{\alpha\beta} + P^C_{\alpha\beta}. \tag{21}$$

The kinetic and configurational contributions to the pressure tensor at a point $\mathbf{R}$ are given by the following expressions:

$$P^K_{\alpha\beta}(\mathbf{R}) = \sum_i m_i v_{i,\alpha} v_{i,\beta} \delta(\mathbf{R} - \mathbf{r}_i), \tag{22}$$

$$P^C_{\alpha\beta}(\mathbf{R}) = -\sum_i \left[\nabla^\alpha_i V(\{\mathbf{r}_i\}) \right] \int_{C_{0i}} \mathrm{d}l_\beta \delta(\mathbf{R} - \mathbf{l}), \tag{23}$$

where m_i, $\mathbf{r}_i$ and $v_{i,\alpha}$ are the mass, the position, and the α-the component of the velocity of the i-th atom, respectively, $V(\{\mathbf{r}_i\})$ is the interaction potential, and C_{0i} is a contour connecting the particle position $\mathbf{r}_i$, with an arbitrary reference point $\mathbf{R}_0$ [43].

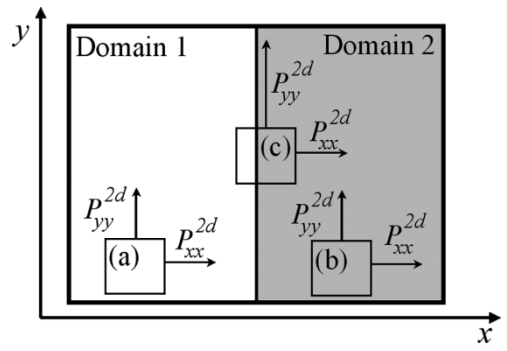

Figure 5. Origin of the line tension between domains 1 and 2 of a bilayer. The 2d pressure tensor is isotropic away from the domain boundary as shown in insets (a) and (b). The anisotropy of the pressure tensor at the domain boundary illustrated in inset (c) leads to the line tension.

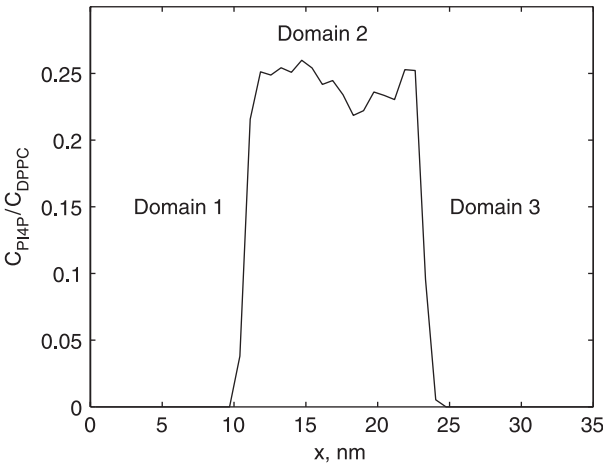

Figure 6. Spatial dependence of the ratio of the bead densities of the PI4P and DPPC lipid molecules in a system used for the line tension calculation. The concentration of PI4P in the mixed PI4P/DPPC domain (domain 2) is 20%.

The kinetic pressure tensor is isotropic and therefore does not contribute to the line tension. Therefore, in what follows we focus on computation of the configurational pressure tensor $P^C(z)$. This tensor is not uniquely defined due to interactions between atoms that are located on the opposite sides of a domain boundary [44]. This ambiguity follows from the arbitrariness in the choice of the contour C_{0i}. In this work, we use the Irving–Kirkwood contour which corresponds to a straight line between interacting particles [45] and use an expression for the configurational pressure tensor for a multi-body potential derived in Ref. [29].

4.2.2 System preparation and simulation details. In order to compute the line tension between pure DPPC bilayers and mixed DPPC/PI4P bilayers, we prepare a system containing one domain of a mixed DPPC/PI4P bilayer sandwiched between two domains of pure DPPC bilayers. An example of PI4P concentration profile of such a system is shown in figure 6. The domain boundaries are parallel to the y-axis and the PI4P molecules are contained within domain 2 of the bilayer. This system was prepared from the homogeneous bilayers that were used in our tilt and splay moduli calculations described in Section 4.1. The equilibrated homogeneous bilayer domains containing 800 lipids each were placed next to each other. The potential energy of the obtained system was then minimized using the steepest descent method for 50,000 steps. Additional water beads were then added to the system to bring the hydration level to 22 coarse-grained water beads per lipid. The potential energy of the hydrated system was then minimized again using the steepest descent method for 50,000 steps.

We observed in our preliminary simulations that PI4P molecules readily diffuse into domains 1 and 3 out of the

PI4P-containing domain 2. In order to keep these domains well-defined and to prevent diffusion of PI4P molecules into the pure DPPC domains of the bilayer, a repulsive wall consisting of "dummy" atoms was constructed. The wall is parallel to the $y-z$ plane and is perpendicular to the lipid bilayer. The "dummy" atoms which constitute the wall interact only with PI4P molecules and do not affect the motion of DPPC and water molecules. The interaction potential between the "dummy" atoms and the PI4P beads is taken to be the repulsive part of the LJ potential for interactions between hydrophobic (C) and hydrophilic (P) beads, i.e.

$$V^{\text{dummy}}(r) = 4\epsilon\left(\frac{r_0}{r}\right)^{12}, \tag{24}$$

where $\epsilon = 1.8$ kJ/mol and $r_0 = 0.47$ nm.

The "dummy" atoms are kept fixed at their positions throughout the simulation and are located on a square grid with 0.5 nm spacing in both y- and z-directions. The x coordinate of the "dummy" atoms corresponding to the wall on the left (right) boundary of domain 2 is equal to coordinate of the left-most (right-most) PI4P bead of domain 2 minus (plus) 0.4 nm. These artificially constructed "dummy" atom walls can be thought of as a simple model for a more complex mechanism (most likely mediated by proteins) preventing PI4P from spreading throughout the entire membrane.

Thus, prepared systems were equilibrated for 400 ns keeping the temperature at 323 K and the pressure at one bar. The equilibration was followed by a 800 ns production run.

Instead of the 2d pressure tensor $P^{2d}(x, y)$ described above, it is more practical to compute an average of the 3d pressure tensor in the direction normal to the bilayer surface, i.e. to replace the limits of integration $[-h, h]$ in equation (19) by the entire vertical span of the simulation box. This removes the ambiguity in the definition of the membrane vertical boundaries ($\pm h$). Since the expanded region of integration contains only the bulk water, this change in the integration boundaries will not affect the values ($P^{2d}_{xx} - P^{2d}_{yy}$) of the difference between the components of the 2d pressure tensor. In addition, the system is uniform in the direction parallel to the domain boundaries (i.e. to the y-axis). Therefore, in what follows we report the x-dependence of the components of the 3d pressure tensor averaged over the y- and z-directions.

4.2.3 Results. Calculation of line tension was conducted for systems with inhomogeneous domains containing 5, 10 and 20% PI4P. Below we show the results for the highest considered concentration, 20% PI4P since the results for the lower PI4P concentrations are very similar. In the analysis the pressure was calculated as a function of the x-direction, which is normal to the boundary between the domains. The contributions of van der Waals, electrostatic, bond length and bond angle vibration forces to the x- and y-components of the pressure tensor are shown in figure 7. It is clear that for all these contributions the x- and y-components are identical up to the statistical error. The result suggests that there is a vanishing line tension between the pure DPPC and mixed PI4P/DPPC domains.

This finding qualitatively agrees with our observation that the DPPC and PI4P molecules freely mix with each other.

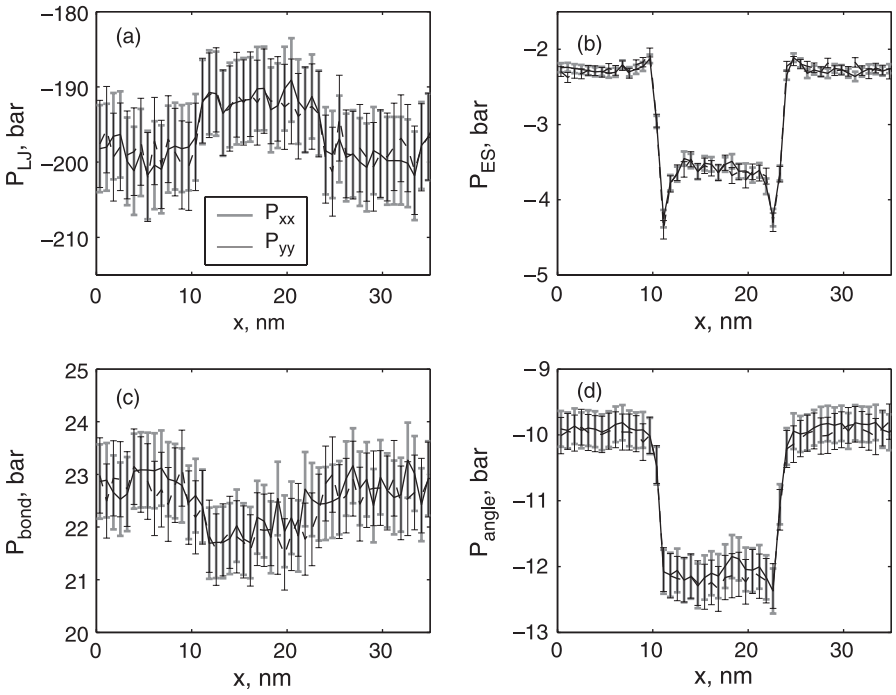

Figure 7. Contribution of various forces to the x- and y-components of the pressure tensor, P_{xx} (grey line) and P_{yy} (black line). Contributions of the LJ, electrostatic (ES), bond and angle potentials to the pressure tensor are shown in plots (a)–(d), respectively.

In other words, there is no significant energetic penalty (which would be manifested in the line tension) for these two molecules to mix.

5. Conclusions

In this work, we developed a systematic approach to compute the three key elastic properties of inhomogeneous lipid bilayers, namely the splay modulus κ, the tilt modulus κ_θ, and the line tension σ between domains of a membrane. We have applied this approach to the analysis of CGMD simulations of mixed DPPC/PI4P bilayers and have observed that addition of PI4P molecules with concentration as high as 20% does not change the elastic properties of DPPC bilayers.

Nevertheless, the obtained results do not rule out a possibility of changes in membrane elastic properties due to a localized formation of lipids. One of the possible reasons for the observed absence of changes in the elastic properties of a DPPC bilayer upon addition of PI4P is an insufficient refinement of the current coarse-grained model. The coarse-grained models for DPPC and water are well established through comparison with experiments and simulations with detailed atomistic models [32]. However, the model for PI4P introduced in this work probably requires further improvements. Since the main goal of this work was to develop the methods to compute the relevant elastic properties for inhomogeneous bilayers, we have chosen a relatively simple model for PI4P using the building blocks provided by the coarse-grained model of Ref. [32]. In particular, in the current work we modeled the rather bulky inositol ring of the PI4P molecule by a single coarse-grained bead of the same radius (0.47 nm) as other beads (figure 1). It perhaps would be more realistic to model the inositol ring by a larger coarse-grained bead. It is expected that a larger headgroup size of the modified PI4P model will introduce an additional stress within the membrane leading to changes in its elastic properties.

Moreover, in the current work we assumed a short-ranged electrostatic potential due to screening, following the model of Ref. [32]. However, since the headgroup of PI4P has a net negative charge not balanced by counterions, it is likely that screening of the electrostatic interactions of the PI4P headgroups is limited. The long range electrostatic interactions will most likely affect the elastic properties of the mixed DPPC/PI4P bilayers.

Finally, it is important to note that PI4P is only one member of the phosphoinositide family and it is well known that phosphoinositides with bulkier headgroups, such as PIP_2 and PIP_3, [4,18] have a more significant impact on the membrane elastic properties.

Acknowledgements

The authors acknowledge the University of Florida High-Performance Computing Center for providing computational resources and support that have contributed to the research results reported within this paper.

References

[1] L.V. Chernomordik, M.M. Kozlov. Protein–lipid interplay in fusion and fission of biological membranes. *Ann. Rev. Biochem.*, **72**, 175 (2003).
[2] R. Schekman, L. Orci. Coat proteins and vesicle budding. *Science*, **271**, 1526 (1996).
[3] J.E. Rothman, F.T. Wieland. Protein sorting by transport vesicles. *Science*, **272**, 227 (1996).
[4] K.N. Burger. Greasing membrane fusion and fission machineries. *Traffic*, **1**, 605 (2000).
[5] R. Lipowsky. Budding of membranes induced by intramembrane domains. *J. Phys. II*, **2**, 1825 (1992).
[6] M.P. Sheetz, S.J. Singer. Biological membranes as bilayer couples. A molecular mechanism of drug–erythrocyte interactions. *Proc. Natl. Acad. Sci. USA*, **71**, 4457 (1974).
[7] E. Farge, D.M. Ojcius, A. Subtil, A. Dautry-Varsat. Enhancement of endocytosis due to aminophospholipid transport across the plasma membrane of living cells. *Am. J. Physiol.*, **276**, C725 (1999).
[8] J.E. Ferrell, W.H. Huestis. Phosphoinositide metabolism and the morphology of human erythrocytes. *J. Cell. Biol.*, **98**, 1992 (1984).
[9] R. Weigert, M.G. Silletta, S. Span, G. Turacchio, C. Cericola, A. Colanzi, S. Senatore, R. Mancini, E.V. Polishchuk, M. Salmona, F. Facchiano, K.N. Burger, A. Mironov, A. Luini, D. Corda. CtBP/BARS induces fission of Golgi membranes by acylating lysophosphatidic acid. *Nature*, **402**, 429 (1999).
[10] A. Schmidt, M. Wolde, C. Thiele, W. Fest, H. Kratzin, A.V. Podtelejnikov, W. Witke, W.B. Huttner, H.D. Sling. Endophilin I mediates synaptic vesicle formation by transfer of arachidonate to lysophosphatidic acid. *Nature*, **401**, 133 (1999).
[11] E.E. Kooijman, V. Chupin, B. de Kruijff, K.N.J. Burger. Modulation of membrane curvature by phosphatidic acid and lysophosphatidic acid. *Traffic*, **4**, 162 (2003).
[12] E.A. Evans, W. Rawicz. Entropy-driven tension and bending elasticity in condensed-fluid membranes. *Phys. Rev. Lett.*, **64**, 2094 (1990).
[13] E. Lindahl, O. Edholm. Mesoscopic undulations and thickness fluctuations in lipid bilayers from molecular dynamics simulations. *Biophys. J.*, **79**, 426 (2000).
[14] S.J. Marrink, A.E. Mark. Effect of undulations on surface tension in simulated bilayers. *J. Phys. Chem. B*, **105**, 6122 (2001).
[15] T.F. Martin. PI(4,5)P(2) regulation of surface membrane traffic. *Curr. Opin. Cell. Biol.*, **13**, 493 (2001).
[16] M. Jost, F. Simpson, J.M. Kavran, M.A. Lemmon, S.L. Schmid. Phosphatidylinositol-4,5-bisphosphate is required for endocytic coated vesicle formation. *Curr. Biol.*, **8**, 1399 (1998).
[17] M. de Matteis, A. Godi, D. Corda. Phosphoinositides and the Golgi complex. *Curr. Opin. Cell. Biol.*, **14**, 434 (2002).
[18] T. Takenawa, T. Itoh. Phosphoinositides, key molecules for regulation of actin cytoskeletal organization and membrane traffic from the plasma membrane. *Biochim. Biophys. Acta*, **1533**, 190 (2001).
[19] J. Bradshaw, R. Bushby, C. Giles, M. Saunders, A. Saxena. The headgroup orientation of dimyristoylphosphatidylinositol-4-phosphate in mixed lipid bilayers: a neutron diffraction study. *Biochim. Biophys. Acta*, **1329**, 124 (1997).
[20] W. Helfrich. Elastic properties of lipid bilayers: theory and possible experiments. *Z. Naturforsch [C]*, **28**, 693 (1973).
[21] U. Seifert, K. Berndl, R. Lipowsky. Shape transformations of vesicles: phase diagram for spontaneous-curvature and bilayer-coupling models. *Phys. Rev. A*, **44**, 1182 (1991).
[22] M. Hamm, M. Kozlov. Tilt model of inverted amphiphilic mesophases. *Eur. Phys. J. B*, **6**, 519 (1998).
[23] M. Hamm, M. Kozlov. Elastic energy of tilt and bending of fluid membranes. *Eur. Phys. J. E*, **3**, 323 (2000).
[24] Y. Kozlovsky, M.M. Kozlov. Stalk model of membrane fusion: solution of energy crisis. *Biophys. J.*, **82**, 882 (2002).
[25] Y. Kozlovsky, M.M. Kozlov. Membrane fission: model for intermediate structures. *Biophys. J.*, **85**, 85 (2003).
[26] F. Jlicher, R. Lipowsky. Shape transformations of vesicles with intramembrane domains. *Phys. Rev. E*, **53**, 2670 (1996).

[27] H. Noguchi, M. Takasu. Fusion pathways of vesicles: a Brownian dynamics simulation. *J. Chem. Phys.*, **115**, 9547 (2001).
[28] D.-W. Li, X.Y. Liu. Examination of membrane fusion by dissipative particle dynamics simulation and comparison with continuum elastic models. *J. Chem. Phys.*, **122**, 174909 (2005).
[29] R. Goetz, R. Lipowsky. Computer simulations of bilayer membranes: self-assembly and interfacial tension. *J. Chem. Phys.*, **108**, 7397 (1998).
[30] J.C. Shelley, M.Y. Shelley, R.C. Reeder, S. Bandyopadhyay, M.L. Klein. A coarse grain model for phospholipid simulations. *J. Phys. Chem. B*, **105**, 4464 (2001).
[31] M.J. Stevens, J.H. Hoh, T.B. Woolf. Insights into the molecular mechanism of membrane fusion from simulation: evidence for the association of splayed tails. *Phys. Rev. Lett.*, **91**, 188102 (2003).
[32] S.J. Marrink, A.H. de Vries, A.E. Mark. Coarse grained model for semiquantitative lipid simulations. *J. Phys. Chem. B*, **108**, 750 (2004).
[33] R. Faller, S.-J. Marrink. Simulation of domain formation in DLPC–DSPC mixed bilayers. *Langmuir*, **20**, 7686 (2004).
[34] B. Smit. Molecular-dynamics simulations of amphiphilic molecules at a liquid–liquid interface. *Phys. Rev. A*, **37**, 3431 (1988).
[35] B.J. Palmer, J. Liu. Simulations of micelle self-assembly in surfactant solutions. *Langmuir*, **12**, 746 (1996).
[36] D. van der Spoel, E. Lindahl, B. Hess, G. Groenhof, A.E. Mark, H.J.C. Berendsen. GROMACS: fast, flexible and free. *J. Comput. Chem.*, **26**, 1701 (2005).
[37] H.J.C. Berendsen, J.P.M. Postma, W.F. van Gunsteren, A. DiNola, J.R. Haak. Molecular dynamics with coupling to an external bath. *J. Chem. Phys.*, **81**, 3684 (1984).
[38] R. Goetz, G. Gompper, R. Lipowsky. Mobility and elasticity of self-assembled membranes. *Phys. Rev. Lett.*, **82**, 221 (1999).
[39] W. Rawicz, K.C. Olbrich, T. McIntosh, D. Needham, E. Evans. Effect of chain length and unsaturation on elasticity of lipid bilayers. *Biophys. J.*, **79**, 328 (2000).
[40] E.R. May, A. Narang, D.I. Kopelevich. Role of molecular tilt in thermal fluctuations of lipid membranes. submitted to *Phys. Rev. Lett.*, (2007).
[41] P.I. Kuzmin, S.A. Akimov, Y.A. Chizmadzhev, J. Zimmerberg, F.S. Cohen. Line tension and interaction energies of membrane rafts calculated from lipid splay and tilt. *Biophys. J.*, **88**, 1120 (2005).
[42] J.P.R.B. Walton, D.J. Tildesley, J.S. Rowlinson, J.R. Henderson. The pressure tensor at the planar surface of a liquid. *Mol. Phys.*, **48**, 1357 (1983).
[43] P. Schofield, J. Henderson. Statistical mechanics of inhomogeneous fluids. *Proc. R. Soc. Lond. A*, **379**, 231 (1982).
[44] J. Sonne, F.Y. Hansen, G.H. Peters. Methodological problems in pressure profile calculations for lipid bilayers. *J. Chem. Phys.*, **122**, 124903 (2005).
[45] J.H. Irving, J.G. Kirkwood. The statistical mechanical theory of transport processes. IV. The equations of hydrodynamics. *J. Chem. Phys.*, **18**, 817 (1950).